

Article

UDC 539.171.016

 <https://doi.org/10.31489/2025PH4/7-15>

Received: 1.06.2025

Accepted: 09.09.2025

D. Soldatkhan¹, A. Morzabayev¹✉, B. Mauey^{1, 2}

¹L.N. Gumilyov Eurasian National University, Astana, Kazakhstan;

²Joint Institute for Nuclear Research, Dubna, Russia

**The analysis of the elastic scattering of the ${}^6\text{He}+{}^{208}\text{Pb}$ nuclear system
using the new B3Y-Fetal potential**

At energies close to the Coulomb barrier, a semi-microscopic analysis of the angular distribution of elastic scattering of the halo nucleus ${}^6\text{He}$ on the heavy nucleus ${}^{208}\text{Pb}$ was performed. In this analysis, the effectiveness of the new B3Y-Fetal folding potential for the large asymmetric ${}^6\text{He}+{}^{208}\text{Pb}$ system was investigated. The effective NN interactions, M3Y and B3Y potentials, were constructed taking into account the distribution features of the weakly bound neutrons of the ${}^6\text{He}$ halo nucleus in the strong Coulomb field of the ${}^{208}\text{Pb}$ nucleus. These density-dependent folding potentials were used as the real part of the optical model potential. The obtained results successfully reproduce the experimental data on elastic scattering. The new B3Y-Fetal potential provides a more accurate description of the NN interaction at large distances in highly asymmetric systems, thereby yielding a more precise prediction of the angular distributions of elastic scattering. The density-dependent modified CDM3Y6-Paris and CDB3Y6-Fetal potentials offer a more realistic description of NN interactions in nuclear matter, since the density-dependent parameters C , α , β , and γ were chosen based on the value of the incompressibility coefficient K calculated at the saturation point. For the ${}^6\text{He}+{}^{208}\text{Pb}$ system at energies $E_{\text{lab}} = 22$ and 27 MeV, a set of optimal parameters for elastic scattering cross sections near the Coulomb barrier was determined. The effectiveness of the new B3Y-Fetal potential in describing the angular distribution of elastic scattering was confirmed. The results of the semi-microscopic analysis are characterized by the renormalization factor N_r and the χ^2/N coefficients. The obtained results may contribute to nuclear astrophysics, particularly to studies of halo nuclei structures and the mechanisms of nuclear interaction processes.

Keywords: elastic scattering, ${}^6\text{He}$ — halo nucleus, ${}^{208}\text{Pb}$ — heavy nucleus, folding potential, B3Y-Fetal, K — incompressibility coefficient

✉ *Corresponding author:* Morzabayev, Aidar, morzabayev_ak@enu.kz

Introduction

The ${}^6\text{He}+{}^{208}\text{Pb}$ system is one of the widely studied topics in modern nuclear physics. Such investigations are important for understanding the structure of exotic nuclei and the mechanisms of their interactions. The ${}^6\text{He}+{}^{208}\text{Pb}$ system also aids in modeling nucleosynthesis processes occurring in stars, which is essential in nuclear astrophysics. Studies involving the ${}^6\text{He}$ nucleus make a significant contribution to understanding neutron density distributions (neutron halo), particularly in providing deeper insight into the r-process [1].

In systems with large asymmetry, effects such as the nuclear rainbow, weak absorption, and pronounced oscillations in the scattering cross section can be observed. The strong Coulomb field of the heavy ${}^{208}\text{Pb}$ nucleus, along with the ability to incorporate the density distribution of weakly bound halo nuclei (such as ${}^6\text{He}$,

^{11}Be , and ^8B), plays an important role in studying their breakup into fragments. This is due to the fact that their neutron halo structure differs significantly from that of standard nuclei [2]. In this regard, a microscopic investigation of the breakup of the ^6He nucleus scattered from a ^{208}Pb target is of great interest.

The elastic scattering of the $^6\text{He}+^{208}\text{Pb}$ system was studied using a microscopic analysis based on the newly developed B3Y(Botswana-3 Yukawa)-Fetal folding potential [2]. We aimed to investigate this system using the double folding model (DFM), which accounts for the nucleon densities of both interacting nuclei. The microscopic effective nucleon-nucleon (NN) interactions, such as the M3Y (Michigan-3-Yukawa) realistic potentials, are constructed by taking into account the nucleon density distributions [3]. Additionally, we aimed to comparatively evaluate our results obtained using the B3Y-Fetal potential against the data reported by other authors [4]. In the folding model, the effective NN interaction potential is constructed microscopically by taking into account the density distribution of nucleons. This approach makes it possible to integrate over the interactions of each nucleon, providing a more accurate description of the mean field inside the nucleus. As a result, the obtained folding potential accounts for the saturation properties of nuclear matter and the density distribution at the nuclear surface. Such features allow for more reliable predictions of the angular distribution in elastic scattering, refinement of nuclear characteristics, and more accurate calculations of reactions. Therefore, the results of such an analysis are of great importance in nuclear astrophysics and thermonuclear energy research.

The halo structure of the ^6He nucleus, characterized by a wide spatial distribution of neutrons, was calculated in the strong field of the heavy ^{208}Pb nucleus, and the results were tested against experimental data. In the study of the $^6\text{He}+^{208}\text{Pb}$ system, the M3Y-Reid, M3Y-Paris, and B3Y-Fetal potentials are modified to more accurately describe the NN interactions within nuclear matter [5].

The delicate balance between the Coulomb and nuclear potentials is clearly manifested in the DFOM (Double Folding Optical Model) framework. The M3Y-Reid, M3Y-Paris, and B3Y-Fetal potentials allow these processes to be described based on realistic density distributions and NN interactions [6]. The approach of using density-dependent potentials is well-suited for the $^6\text{He}+^{208}\text{Pb}$ system, as it provides a better opportunity to account for the diffuse density characteristic of the halo structure [7]. In the folding model, realistic NN interactions are combined with accurate nuclear matter density functions, offering a more precise description [8]. The difference between this work and the studies by Khoa et al. lies in the use of the new B3Y-Fetal potential for the NN interaction and the introduction of density-dependent parameters into this potential.

The new B3Y-Fetal potential differs from the traditional M3Y-Reid and M3Y-Paris potentials in that it is derived from the calculation of nuclear matrix elements of the two-body interaction within the variational method with lowest-order constraints (LOCV) [2]. In semi-microscopic analysis, the accuracy of the folding potential is determined by the renormalization coefficient N_r . The coefficient N_r is obtained during calculations with the FRESKO code by comparing theoretical cross sections with experimental data. The closer the value of N_r is to 1, the more accurately the applied folding potential describes the real nuclear force. Meanwhile, the χ^2/N comparison coefficient reflects the degree of agreement between the calculated and experimental cross sections. The combination of these two parameters makes it possible to assess the reliability of the folding potential.

The main reason why the B3Y-Fetal potential provides good results is that, when introducing corrections to the density-dependent formula, it takes into account the saturation density of the binding forces in the nuclear medium, namely the incompressibility coefficient K . From a physical point of view, this model can be explained as follows: first, the calculation is performed from the center of the ^6He nucleus based on the nucleon density distribution of the ^{208}Pb nucleus. Second, the calculation is performed from the center of the ^{208}Pb nucleus based on the nucleon density distribution of the ^6He nucleus. For this reason, the method is called the double-folding model

The two-parameter density model (Fermi or Woods–Saxon) describes the nucleus in a simple form through the central density distribution and the surface thickness (radius, diffuseness). In contrast, in the DFM, the nucleon density distributions of two nuclei ($\rho_1(r_1)$, $\rho_2(r_2)$) are taken and folded with the effective NN interaction to construct a fully microscopic potential. In other words, this is a more complex microscopic method that takes into account the complete density distribution of both nuclei, rather than just one. Cluster models (for example, α -cluster models) play an important role in describing the correlation of nucleons inside the nucleus and their grouped interactions. For instance, DWBA is used in reaction theory models to describe inelastic processes (transfer reactions) in nuclear reactions. In the future, just as we have applied this approach to other systems, we will also apply it to the $^6\text{He}+^{208}\text{Pb}$ system.

As a result of this study, the elastic scattering of the ${}^6\text{He}+{}^{208}\text{Pb}$ system is successfully described based on density-dependent folding potentials. The weakly bound nature of the halo-structured ${}^6\text{He}$ nucleus provides deeper insight into the specific features of nucleus–nucleus interactions. This not only expands the boundaries of nuclear physics but also enhances the accuracy of astrophysical models.

Theoretical formalisms and procedures

Based on the DFM, a modified effective NN interaction potential (M3Y) is obtained by taking into account the nucleon density distributions of the ${}^6\text{He}+{}^{208}\text{Pb}$ system. The resulting folding potential constitutes the real part of the optical potential (OP). Using this OP, we evaluate the accuracy of the theoretical model by describing the angular distribution of elastic scattering in comparison with experimental data on nucleus–nucleus interactions.

Since ${}^6\text{He}$ is a weakly bound nucleus prone to breakup, it induces a pronounced cluster structure of neutrons and alpha particles at energies near the strong Coulomb barrier of the ${}^{208}\text{Pb}$ nucleus [9]. Therefore, to clarify the pure elastic scattering cross sections of neutrons, an analysis was carried out at near-barrier energies of $E_{\text{lab}} = 22$ and 27 MeV. The nucleus–nucleus realistic potential is obtained in the following form [10].

$$V(R) = \iint \rho_{6\text{He}}(\vec{r}_1) \rho_{208\text{Pb}}(\vec{r}_2) \mathfrak{V}_{\text{NN}}(|\vec{R} + \vec{r}_2 - \vec{r}_1|) d^3r_1 d^3r_2 \quad (1)$$

Here, \mathfrak{V}_{NN} is the effective NN interaction potential of the M3Y type.

The formula for calculating the direct and exchange parts of the NN effective interaction based on the M3Y-Reid potential is given in [11].

$$v_D(s) = 7999.0 \frac{e^{-4s}}{4s} - 2134.25 \frac{e^{-2.5s}}{2.5s} \quad (2)$$

$$v_{EX}(s) = 4631.4 \frac{e^{-4s}}{4s} - 1787.1 \frac{e^{-2.5s}}{2.5s} - 7.8474 \frac{e^{-0.7072s}}{0.7072s} \quad (3)$$

for M3Y-Paris potential [11]:

$$v_D(s) = 11061.6 \frac{e^{-4s}}{4s} - 2537.5 \frac{e^{-2.5s}}{2.5s} \quad (4)$$

$$v_{EX}(s) = -1524.0 \frac{e^{-4s}}{4s} - 518.8 \frac{e^{-2.5s}}{2.5s} - 7.8474 \frac{e^{-0.7072s}}{0.7072s} \quad (5)$$

for the new B3Y-Fetal potentials [12]:

$$v_D(s) = 10472.13 \frac{e^{-4s}}{4s} - 2203.11 \frac{e^{-2.5s}}{2.5s} \quad (6)$$

$$v_{EX}(s) = 499.63 \frac{e^{-4s}}{4s} - 1347.77 \frac{e^{-2.5s}}{2.5s} - 7.8474 \frac{e^{-0.7072s}}{0.7072s} \quad (7)$$

The B3Y and M3Y type potentials are modified to be dependent on both energy and density [13].

$$v_{D(EX)}(\rho, r, s) = F(E, \rho) g(E) v'_{D(EX)}(s) \quad (8)$$

The density-dependent function ($F(\rho)$) is given as [14]:

$$F(\rho) = C(1 + \alpha e^{-\beta\rho}) - \gamma\rho \quad (9)$$

The energy-dependent factor ($g(E)$) is given as [14]:

$$g(E) = (1 - 0.003E / A) \quad (10)$$

The density-dependent parameters are chosen to reduce the K-value in accordance with the saturation property of nuclear matter (as shown in Table 1). The CDM3Y6 parameters were applied to the B3Y-Fetal potential to construct the CDB3Y6-Fetal version.

The parameters of the M3Y-Reid, M3Y-Paris, and B3Y-Fetal potentials are presented [10]

Density dependence	C	α	β (fm ³)	γ (fm ³)	K (MeV)
CDM3Y6-Reid CDM3Y6-Paris CDB3Y6-Fetal	0.2658	3.8033	1.4099	4.0	252

In the region near the saturation point, the curvature of the binding energy per nucleon curve depends on the K — incompressibility of nuclear matter [10].

The nuclear compressibility coefficient is calculated using the following equation [11]:

$$K_{\infty} = -\frac{3\hbar^2 k_F^3}{5m} + 5J_D C \beta(\varepsilon) \rho_{\rho=\rho_0}^{5/3} \quad (11)$$

The dependence curve of the binding energy per nucleon on the nuclear matter density allows for the determination of the actual saturation density ρ_0 of the nucleus [15]. The saturation density ρ_0 represents the density per unit volume that characterizes the “natural” arrangement of nucleons inside the nucleus where the binding energy reaches its maximum value. In this case, the binding energy of nuclear matter can be approximated in the following form [16].

$$\frac{B}{A}(\rho) = a_V \left(1 - \frac{1}{2} \left(\frac{\rho - \rho_0}{\rho_0} \right)^2 \right), \quad (12)$$

where $\frac{B}{A}$ is the binding energy per nucleon; ρ is the nuclear matter density; ρ_0 is the saturation density, and a_V is the volume binding energy coefficient. To find the point where the binding energy reaches its maximum, we write it in the following form.

$$\frac{d\left(\frac{B}{A}\right)}{d\rho} = 0. \quad (13)$$

For the ²⁰⁸Pb nucleus, the normal saturation density has a value of approximately $\rho_0 \approx 0.16 \text{ fm}^{-3}$, according to both experimental and theoretical studies [17].

Determining the exact saturation density for the ⁶He nucleus is a special case, as it has a halo structure composed of ${}^6\text{He} \rightarrow 4\text{He} + 2n$. The two neutrons are spatially extended away from the core, meaning its structure is characterized by a broadly distributed, diffuse density. This expands its overall density distribution, reduces the average density, and the corresponding calculated results can be approximated using the following formula [18].

$$\rho_{6\text{He}} = \frac{A}{\frac{4}{3}\pi R^3} \approx 0.09 \text{ fm}^{-3} \quad (14)$$

Here, R is the mean radius of the nucleus. For ⁶He, the experimental radius is approximately $R \approx 2.5 \text{ fm}$, with mass number $A = 6$.

We express the nucleon density distribution of each colliding nucleus using the two-parameter Fermi (2pF) model [19] and the result of the calculation is shown in the following Table 2:

$$\rho(r) = \frac{\rho_0}{1 + \exp\left(\frac{r-c}{z}\right)}. \quad (15)$$

Table 2

2pF-model, $c, z, \langle r^2 \rangle^{1/2}, \rho_0$ — parameters of the distribution of substance density of the nucleus [19]

Nuclear	$c, \text{ fm}$	$z, \text{ fm}$	$\langle r^2 \rangle^{1/2}, \text{ fm}$	$\rho_0, \text{ fm}^{-3}$
⁶ He	1.8	0.75	2.5	0.08
²⁰⁸ Pb	6.624	0.549	5.521	0.16

Analysis Section

Folding potentials were calculated in the DF POT code. Semi-microscopic analysis was carried out using the FRESKO code [20]. For the ${}^6\text{He}+{}^{208}\text{Pb}$ system at $E_{\text{lab}}=22.0$ MeV, the calculated DF potentials using CDM3Y6-Reid, CDM3Y6-Paris, and CDB3Y6-Fetal interactions are shown in Figure 1.

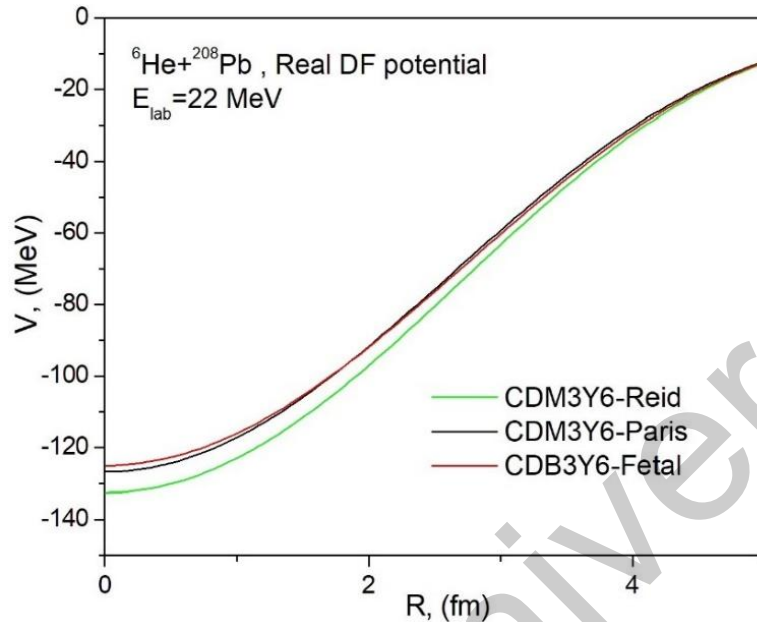


Figure 1. The generated real DF potentials for the ${}^6\text{He}+{}^{208}\text{Pb}$ system at $E_{\text{lab}} = 22.0$ MeV

The depth and characteristics of the DF microscopic potentials obtained for our ${}^6\text{He}+{}^{208}\text{Pb}$ system are consistent with the results reported in the literature [21]. Due to the large asymmetry in the ${}^6\text{He}+{}^{208}\text{Pb}$ system, constructing the CDM3Y6-Reid, CDM3Y6-Paris, and CDB3Y6-Fetal potentials within the DFM was challenging. It was observed that the CDM3Y6-Paris and CDB3Y6-Fetal potentials, being density-dependent, are noticeably deeper in the radial regions up to 3 fm.

Table 3

OM and DFOM parameters for the ${}^6\text{He}+{}^{208}\text{Pb}$ elastic scattering at $E_{\text{lab}} = 22.0$ MeV and $E_{\text{lab}} = 27.0$ MeV energy, $r_c = 1.25$ fm

E MeV	Model	Type of real potential				Imaginary potential parameter (WS)				σ_R mb
		V_0 MeV	Rv fm	av fm	N_r	W_0 MeV	r_w fm	a_w fm	χ^2/N	
22.0	OM Exp: [22, 23,24]	170.7	0.9	0.55	–	20.4	1.4	0.74	0.77 2.0 2.89	1099
	DFOM	CDM3Y6- Reid			0.79	20.4	1.4	0.74	–	1357
	DFOM	CDM3Y6-Paris			0.8	20.4	1.4	0.74	–	1378
	DFOM	CDB3Y6- Fetal			0.85	20.4	1.4	0.74	–	1365
27.0	OM (для exp: [25])	170.7	0.9	0.55	–	20.4	1.4	0.74	0.06	1940
	DFOM	CDM3Y6-Paris			0.8	20.4	1.4	0.74	–	1876
	DFOM	CDB3Y6- Fetal			0.84	20.4	1.4	0.74	–	2011

Based on the experimental data at $E_{\text{lab}} = 22$ MeV from references [22–24], a common optimal set of parameters was obtained within the framework of the OM analysis (Table 3). The value of χ^2/N -indicates the relative error between the theoretical calculation and the experimental data of the angular distribution for elastic scattering.

The result of the OM analysis is shown in the following Figure 2.

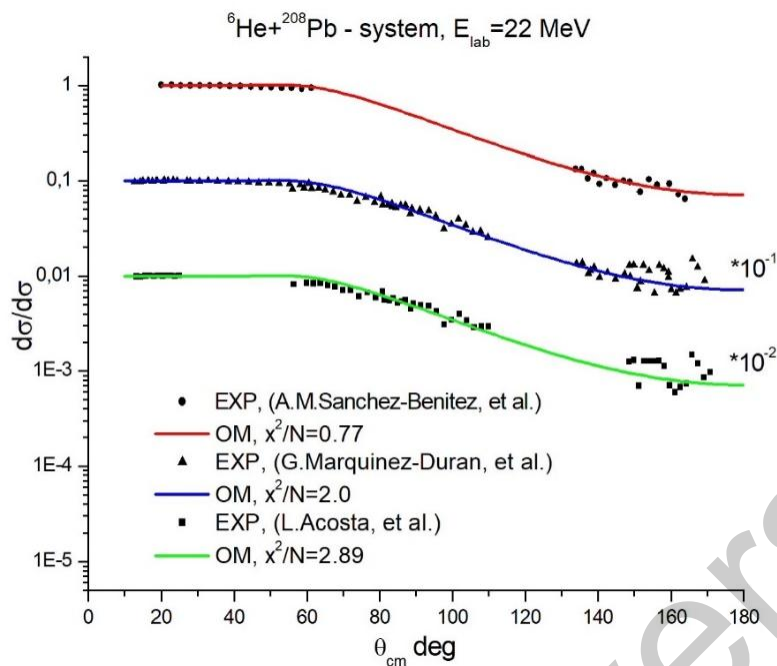


Figure 2. OM results of the ${}^6\text{He}+{}^{208}\text{Pb}$ system at $E_{\text{lab}} = 22$ MeV

In the following analysis, we replace only the real part of these refined OM parameters with a microscopic folding potential. In this semi-microscopic analysis, the parameters of the imaginary part (W_0 , r_w , a_w) remain in the Woods–Saxon form. The stability of the imaginary parameters in the DFOM analysis confirms the reliability of the tested DF real potential. The results of the DFOM model analysis for the experimental data at $E_{\text{lab}} = 22$ MeV [22] and $E_{\text{lab}} = 27$ MeV [25] are presented in Figure 3.

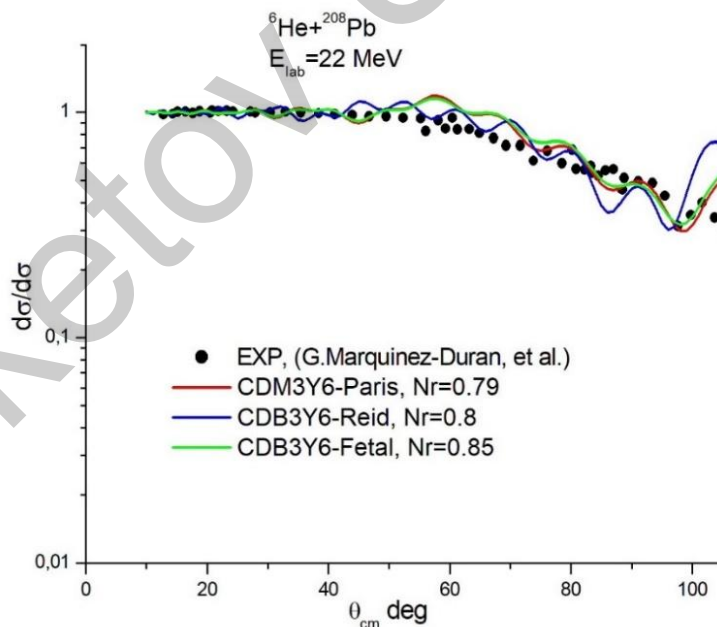


Figure 3. DFOM results of the ${}^6\text{He}+{}^{208}\text{Pb}$ system at $E_{\text{lab}} = 22$ MeV

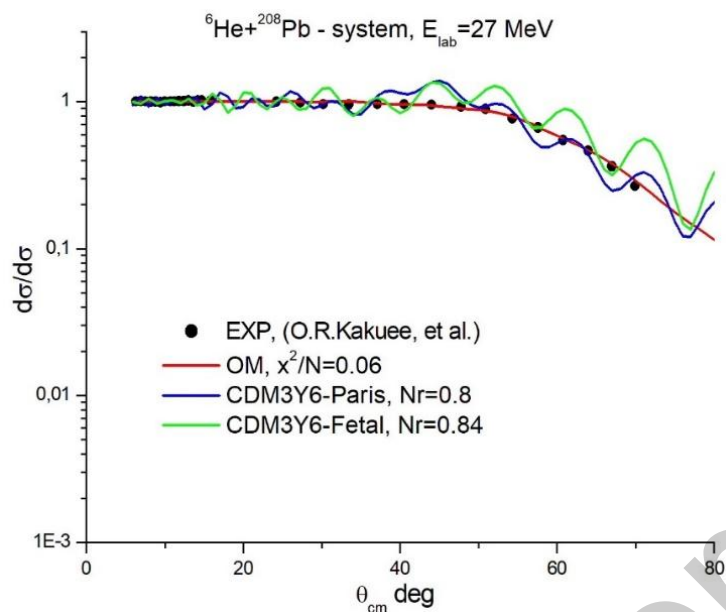


Figure 4. OMa and DFOM results of the ${}^6\text{He}+{}^{208}\text{Pb}$ system at $E_{\text{lab}} = 27$ MeV

In the semi-microscopic analysis, the DF real potential primarily influences the angular distribution of elastic scattering at forward angles (up to 90°). At energies near the Coulomb barrier, cluster transfer effects in the elastic scattering distribution are clearly observed at angles between 60° and 80° . Correspondingly, the density-dependent CDM3Y6-Paris and CDB3Y6-Fetal potentials provided a successful description of this behavior (Figs. 3 and 4). To characterize nuclear reactions and to verify the accuracy of the performed calculations, the σ_R - total reaction cross-sections were determined.

Conclusion

The angular distributions of elastic scattering for the ${}^6\text{He}+{}^{208}\text{Pb}$ system near the Coulomb barrier at $E_{\text{lab}} = 22$ and 27 MeV were analyzed using the DFOM model. Real folding potentials CDM3Y6-Paris and CDB3Y6-Fetal were constructed based on neutron density distributions for this system. The obtained potentials account for the density distribution of the weakly bound neutrons in the ${}^6\text{He}$ halo nucleus in the presence of the strong Coulomb field of the ${}^{208}\text{Pb}$ nucleus.

The density-dependent modified M3Y-Paris and B3Y-Fetal potentials contribute to a more accurate description of nucleon-nucleon interactions in nuclear matter. The structures observed in the angular distributions were successfully explained by the characteristics of these potentials and were evaluated using adjustable normalization coefficients — Nr. A distinctive feature of the DF real potentials was their consideration of the asymmetric nature of the studied system and the calculation at energies near the Coulomb barrier.

In this study, the newly developed CDB3Y6-Fetal potential was successfully applied to the ${}^6\text{He}+{}^{208}\text{Pb}$ nuclear system, which exhibits significant asymmetry in terms of mass and isotopic composition. The effectiveness of this new potential in describing the angular distribution of elastic scattering was demonstrated. Such research results can contribute to nuclear astrophysics, particularly in studying the structure of halo nuclei and the mechanisms of nuclear interaction processes.

Acknowledgment

This research has been funded by the Science Committee of the Ministry of Science and Higher Education of the Republic of Kazakhstan (Grant No. AP13268907).

References

- 1 Arnould, M., Goriely, S., & Takahashi, K. (2007). The r-process of stellar nucleosynthesis: Astrophysics and nuclear physics achievements and mysteries. *Physics Reports*, 450(4–6), 97–213. <https://doi.org/10.1016/j.physrep.2007.06.002>
- 2 Fiase, J.O., Devan, K.R.S., & Hosaka, A. (2002). Mass dependence of M3Y-type interactions and the effects of tensor correlations. *Physical Review C*, 66(1), 014004. <https://doi.org/10.1103/PhysRevC.66.014004>.

- 3 Khoa, D.T., et al. (2007). Folding model analysis of elastic and inelastic ${}^6\text{He}+{}^{208}\text{Pb}$ scattering and the halo structure of ${}^6\text{He}$. *Nuclear Physics A*, 759, 3–30.
- 4 Khoa, D.T., Cuong, D.C., & Loan, D.T. (2023). New density-dependent M3Y interactions for nucleus–nucleus optical potentials and elastic scattering of ${}^6\text{He}$ on ${}^{208}\text{Pb}$. *Nuclear Physics A*, 1035, 122717.
- 5 Amangeldi, et al. (2024). Efficiency of the new B3Y-fetal potential in the analysis of the elastic and inelastic angular distributions for the ${}^{10}\text{B}+{}^{12}\text{C}$ system. *Pramana*, 98(3), 106. <https://doi.org/10.1007/s12043-024-02760-z>.
- 6 Soldatkhan, D., Amangeldi, N., Makhanov, K.M., & Smagulov, Zh.K. (2023). Application of the new B3Y-Fetal potential in the semi-microscopic analysis of the scattering of accelerated ${}^6\text{Li}$ — lithium and ${}^{16}\text{O}$ — oxygen nuclei from the ${}^{12}\text{C}$ — carbon nucleus. *Eurasian Physical Technical Journal*, 25, 4(46), 22–30. <https://doi.org/10.31489/2023No4/17-22>
- 7 Keeley, N., Alamanos, N., Lapoux, V., & Rusek, K. (2009). Review of reactions with light exotic nuclei. *Progress in Particle and Nuclear Physics*, 63(2), 396–447. <https://doi.org/10.1016/j.pnpnp.2009.05.001>
- 8 Amangeldi, N., et al. (2024). Recent Measurement and Theoretical Analysis for the Elastic Scattering of the ${}^{15}\text{N}+{}^{11}\text{B}$ System. *Brazilian Journal of Physics*, 54(5), 169. <https://doi.org/10.1007/s13538-024-01547-2>
- 9 Descouvemont, P. & Hussein, M.S. The cluster structure of ${}^6\text{He}$ and reactions with heavy targets. *Physics Letters B*, 693(6), 568–572 (2010). <https://doi.org/10.1016/j.physletb.2010.09.011>
- 10 Kyoungsu Heo et al. (2024). Folding potential with modern nuclear density functionals and application to ${}^{16}\text{O}+{}^{208}\text{Pb}$ reaction. *Phys. Rev. C*, 110(3), 034616. DOI: <https://doi.org/10.1103/PhysRevC.110.034616>
- 11 Soldatkhan, D., Yergaliuly, G., Amangeldi, N., Mauey, B., Odsuren, M., Awad, Ibraheem A., & Hamada, Sh. (2022). New Measurements and theoretical analysis for the ${}^{16}\text{O}+{}^{12}\text{C}$ Nuclear System. *Brazilian Journal of Physics*, 52(152), 1–10. <https://doi.org/10.1007/s13538-022-01153-0>.
- 12 Soldatkhan, D., Amangeldi, N., Baltabekov, A., & Yergaliuly, G. (2022). Investigation of the energy dependence of the interaction potentials of the ${}^{16}\text{O}+{}^{12}\text{C}$ nuclear system with a semi-microscopic method. *Eurasian Physical Technical Journal*, 19, 3(41), 39–44. <https://doi.org/10.31489/2022No3/39-44>
- 13 AA, B. (2025). Analysis of the effect of the B3Y-fetal potential on energy near the coulomb barrier for the ${}^9\text{Be}+{}^{12}\text{C}$ system. *Eurasian Physical Technical Journal*, 22(1).
- 14 Soldatkhan, D., Mauey, B., Baratova, A.A., & Makhanov, K.M. (2025). Introduction of a New B3Y-Fetal Potential in the Semimicroscopic Analysis of the ${}^{15}\text{N}+{}^{27}\text{Al}$ Nuclear System. *Bulletin of the University of Karaganda — Physics*, 117(1), 29–36.
- 15 Khoa, D.T., von Oertzen W., Bohlen, H.G., & Ohkubo, S. (2007). Nuclear rainbow scattering and nucleus–nucleus potential. *Journal of Physics G: Nuclear and Particle Physics*, 34(5), R111. <https://doi.org/10.1088/0954-3889/34/5/R01>
- 16 Khoa, D.T., Satchler, G.R., & von Oertzen, W. (1997). Nuclear incompressibility and density dependent nucleon–nucleon interaction. *Physics Review C*, 56, 954. <https://doi.org/10.1103/PhysRevC.56.954>
- 17 Ring, P. & Schuck, P. (1980). *The Nuclear Many-Body Problem*. Springer-Verlag, ISBN: 978-3-540-21206-5
- 18 Jensen, A.S., Riisager, K., Fedorov, D.V., & Garrido, E. (2004). Structure and reactions of quantum halos. *Rev. Mod. Phys.* 76, 215. <https://doi.org/10.1103/RevModPhys.76.215>
- 19 de Vries, H., de Jager, C. W., & de Vries, C. (1987). Nuclear charge-density-distribution parameters from elastic electron scattering. *Atomic Data and Nuclear Data Tables*, 36, 495–536.
- 20 Thompson, I.J. (1988). Coupled reaction channels calculations in nuclear physics. *Computer Physics Reports*, 7, 167–212.
- 21 Awad, A. Ibraheem, El-Azab, M.A., & El-Ghafar, H.H. (2021). Analysis of ${}^{4,6,8}\text{He}+{}^{208}\text{Pb}$ elastic scattering using different density-dependent interactions within the double-folding optical model. *International Journal of Modern Physics E*, 30(12), 2150105. <https://doi.org/10.1142/S0218301321501057>
- 22 Sánchez-Benítez, A.M., et al. (2008). Study of the elastic scattering of ${}^6\text{He}$ on ${}^{208}\text{Pb}$ at energies around the Coulomb barrier. *Nuclear Physics A*, 803(1–2), 30–45. <https://doi.org/10.1016/j.nuclphysa.2008.01.015>
- 23 Marquín-Durán, et al. (2016). Precise measurement of near-barrier ${}^8\text{He}+{}^{208}\text{Pb}$ elastic scattering: Comparison with ${}^6\text{He}$. *Physical Review C*, 94(6), 064618. <https://doi.org/10.1103/PhysRevC.94.064618>
- 24 Acosta, L., et al. (2011). Elastic scattering and α -particle production in ${}^6\text{He}+{}^{208}\text{Pb}$ collisions at 22 MeV. *Physical Review C*, 84(4), 044604. <https://doi.org/10.1103/PhysRevC.84.044604>
- 25 Kakuee, O. R., et al. (2004). Long range absorption in the scattering of ${}^6\text{He}$ on ${}^{208}\text{Pb}$ and ${}^{197}\text{Au}$ at 27 MeV. *Nuclear Physics A*, 735(3–4), 321–340. <https://doi.org/10.1016/j.nuclphysa.2004.01.139>

Д. Солдатхан, А.К. Морзабаев, Б. Мауей

${}^6\text{He}+{}^{208}\text{Pb}$ ядролық жүйесінің серпімді шашырауын жаңа ВЗҮ-Fetal потенциалы арқылы талдау

Кулондық тосқауылға жақын энергияларда ${}^6\text{He}$ гало ядроның ${}^{208}\text{Pb}$ ауыр ядросымен серпімді шашырауының бұрыштық таралуына жартылай микроскопиялық талдау жүргізілді. Талдау барысында жаңа ВЗҮ-Fetal фолдинг потенциалдың ${}^6\text{He}+{}^{208}\text{Pb}$ асимметриясы үлкен жүйе үшін тиімділігі зерттелді. Тиімді NN өзара әрекеттесу МЗҮ және ВЗҮ потенциалдары ${}^{208}\text{Pb}$ ядроның күшті кулондық өрісіндегі

${}^6\text{He}$ гало ядроның әлсіз байланысқан нейтрондар тығыздығының таралу ерекшелігін ескеру негізінде құрылды. Тығыздыққа тәуелді бұл фолдинг потенциалдар оптикалық модельдің нақты бөлігі ретінде қолданылды. Алынған талдау нәтижелер серпімді шашыраудың эксперименттік деректерін сәтті сипаттай алды. Жаңа ВЗҮ-Fetal потенциалы асимметриясы үлкен жүйелердегі үлкен қашықтықтарда ядролар арасындағы өзара әрекеттесуді дәлірек сипаттап, серпімді шашыраудың бұрыштық таралуын нақты болжауға мүмкіндік береді. Тығыздыққа тәуелді модификацияланған CDM3Y6-Paris, CDB3Y6-Fetal потенциалдары ядролық материя нуклондарының өзара әсерін барынша нақты сипаттауға үлес қосады. Себебі тығыздығына тәуелді C , α , β , γ — параметрлер қанықтылық нүктесіне қатысты есептелген K сығылмаушылық коэффициенті мәніне байланысты таңдалды. Кулондық тосқауылға жақын $E_{\text{lab}} = 22$ және 27 MeV энергияларда ${}^6\text{He}+{}^{208}\text{Pb}$ жүйесі үшін серпімді шашырау кимасына арналған оңтайлы параметрлер жиынтығы анықталды. Серпімді шашыраудың бұрыштық таралуын сипаттауда жаңа ВЗҮ-Fetal потенциалдың тиімділігі айқындалды. Жартылай микроскопиялық талдау нәтижесін N_r — ренормализация факторы мен χ^2/N — коэффициенттері көрсетеді. Алынған нәтижелері ядролық астрофизикада, әсіресе гало ядроларының құрылымын және ядролық өзара әрекеттесу процестерінің механизмдерін зерттеуге үлес қоса алады.

Кілт сөздер: серпімді шашырау, ${}^6\text{He}$ — гало ядро, ${}^{208}\text{Pb}$ — ауыр ядро, фолдинг потенциалы, ВЗҮ-Fetal, K — сығылмаушылық коэффициенті

Д. Солдатхан, А.К. Морзабаев, Б. Мауей

Анализ упругого рассеяния ядерной системы ${}^6\text{He}+{}^{208}\text{Pb}$ с использованием нового потенциала ВЗҮ-Fetal

При энергиях, близких к кулоновскому барьеру, проведён полумикроскопический анализ угловых распределений упругого рассеяния ядра-гало ${}^6\text{He}$ на ядре ${}^{208}\text{Pb}$. В рамках исследования применён новый фолдинг потенциал ВЗҮ-Fetal для описания асимметричной системы ${}^6\text{He}+{}^{208}\text{Pb}$. Эффективные нуклон-нуклонные взаимодействия в потенциалах МЗҮ и ВЗҮ построены с учётом распределения плотности слабо связанных нейтронов в ${}^6\text{He}$ в кулоновском поле ядра ${}^{208}\text{Pb}$. Зависимые от плотности фолдинг потенциалы использовались в качестве реальной части оптической модели и позволили успешно воспроизвести экспериментальные данные по упругому рассеянию. Показано, что новый потенциал ВЗҮ-Fetal обеспечивает более точное описание взаимодействия ядер на больших расстояниях в сильно асимметричных системах и даёт надёжное предсказание угловых распределений упругого рассеяния. Модифицированные потенциалы CDM3Y6-Paris и CDB3Y6-Fetal вносят вклад в более корректное описание нуклон-нуклонных взаимодействий в ядерной материи, поскольку параметры C , α , β , γ выбирались в зависимости от коэффициента сжимаемости K , рассчитанного вблизи точки насыщения. Для системы ${}^6\text{He}+{}^{208}\text{Pb}$ при энергиях $E_{\text{lab}} = 22$ и 27 МэВ определены оптимальные параметры сечения упругого рассеяния, что подтвердило эффективность потенциала ВЗҮ-Fetal. Результаты полумикроскопического анализа отражаются коэффициентами перенормировки N_r и χ^2/N . Полученные результаты могут внести вклад в ядерную астрофизику, в частности в изучение структуры гало-ядер и механизмов процессов ядерного взаимодействия.

Ключевые слова: упругое рассеяние, ${}^6\text{He}$ — гало-ядро, ${}^{208}\text{Pb}$ — тяжелое ядро, фолдинг потенциал, ВЗҮ-Fetal, K — коэффициент несжимаемости

Information about the authors

Soldatkhon, Dauren — PhD, Senior Teacher, L.N. Gumilyov Eurasian National University, Astana, Kazakhstan; e-mail: soldathan.dauren@gmail.com. SCOPUS Author ID: 57768566200; ORCID ID <https://orcid.org/0000-0001-7981-4100>

Morzabayev, Aidar (*corresponding author*) — Candidate of Physico-Mathematical Sciences, Associate Professor, L.N. Gumilyov Eurasian National University, Astana, Kazakhstan; e-mail: morzabayev_ak@enu.kz; SCOPUS Author ID 26531512300; ORCID ID: <https://orcid.org/record/DJU-9592-2022>

Mauey, Bahytbek — PhD, Senior Teacher, Joint Institute for Nuclear Research, Dubna, Russia; L.N. Gumilyov Eurasian National University, Astana, Kazakhstan; e-mail: bahytbek01@yandex.kz. SCOPUS Author ID: 57193847043; ORCID ID: <https://orcid.org/0000-0003-4301-1327>